Current Research in Microbial Sciences 7 (2024) 100260

Contents lists available at ScienceDirect

Current Research in Microbial Sciences

journal homepage: www.sciencedirect.com/journal/current-research-in-microbial-sciences

ADS-J21 is a novel HIV-1 entry inhibitor targeting gp41

Ruiying Liang [a,1], Dou Dou [a,1], Chunying Wang [b,1], Shanshan Huo [a], Yang Wu [a], Juan Wang [a], Zhengsen Yu [a], Shuomin Zhang [b], Jingjing Xu [b], Yue Liu [c], Peng Liu [a], Shibo Jiang [d,*], Fei Yu [a,*]

[a] Hebei Key Laboratory of Analysis and Control of Zoonotic Pathogenic Microorganism, College of Life Sciences, Hebei Agricultural University, Baoding, 071001, China
[b] Baoding Maternal and Child Health Hospital, Baoding, 071023, China
[c] Department of Biochemistry and Biophysics, University of California, San Francisco, 94158, USA
[d] Shanghai Institute of Infectious Diseases and Biosecurity, Shanghai Medical College, Fudan University, Shanghai, 200032, China

ARTICLE INFO

Keywords:
HIV-1
gp41
Small molecule
Inhibitors
Broad-spectrum

ABSTRACT

HIV-1 envelope glycoprotein gp41 mediates fusion between HIV-1 and host cell membranes, making inhibitors of gp41 attractive anti-HIV drugs. We previously reported an efficient HIV-1 fusion inhibitor, ADS-J1, with a Y-shaped structure. Here, we discovered a new compound, ADS-J21, with a Y-shaped structure similar to that of ADS-J1 but with a lower molecular weight. Moreover, ADS-J21 exhibited effective anti-HIV-1 activity against divergent HIV-1 strains *in vitro*, including several HIV-1 laboratory-adapted strains and primary isolates with different subtypes (clades A to F) and tropisms (X4 or R5). Mechanistic studies have demonstrated that ADS-J21 blocks the formation of the gp41 six-helix bundle (6-HB) by targeting conserved amino acids Lys35 and Trp32. These findings suggest that ADS-J21 can be used as a new lead compound for further optimization in the development of a small-molecule fusion inhibitor.

1. Introduction

Acquired immune deficiency syndrome (AIDS) is caused by infection from the human immunodeficiency virus (HIV), which has become one of the deadliest infectious killers of adults worldwide. Globally, approximately 38.4 million individuals are living with HIV, and 28.7 million people are receiving antiretroviral therapy (ART) (https://www.who.int/hiv/data/en/).

HIV type 1 (HIV-1) entry into the host cells is mediated by its two envelope glycoproteins (Env), gp120 and gp41 (Berger, 1997; Chan and Kim, 1998). In the state of non-fusion, gp120 interacts with gp41 remains noncovalently and oligomerizes as trimers on the surface of the HIV-1 virion (Chan and Kim, 1998). The unliganded gp120 is in a conformational equilibrium, with its core having a strong intrinsic tendency to adopt the CD4-bound conformation (Kwon et al., 2012). This propensity is modulated by gp41 non-covalent interaction and the V1/V2 and V3 variable loops (Huang et al., 2005). After the fusion triggering, HIV-1 gp120 contains 5 disulfide-bonded loop structures that bind to the receptor CD4 V1-V4 loop and a coreceptor CXCR4 or CCR5 (Chan and Kim, 1998; Dimitrov, 1997; Yu et al., 2013), leading to the conformation change of gp41 (Capon and Ward, 1991). Then fusion peptide (FP) in gp41 inserts into the target cell membrane, leading to exposure of its N- and C-terminal heptad repeat (NHR and CHR) (Pancera et al., 2010). Subsequently, the CHR interacts with the NHR to form an antiparallel six-helix bundle (6-HB) core structure that brings viral and cell membranes close for fusion (Chan et al., 1997; Chan and Kim, 1998; Lu et al., 1995; Weissenhorn et al., 1997; Yu et al., 2013). Therefore, gp41 has been recognized as a promising target for the development of anti-HIV drugs, owing to its key role in the early steps of HIV-1 entry into the target cells (Bernstein et al., 1995; Poumbourios et al., 1997).

Enfuvirtide (T-20), the first HIV fusion inhibitor-based peptide drug was approved by the U.S. Food and Drug Administration (FDA) for the treatment of HIV-infected patients who have failed to respond to the HIV replication inhibitor-based anti-HIV drugs (Leal et al., 2023; Pan et al., 2009a,b). Despite its major success, several shortcomings remain for peptide drugs, including a lack of oral bioavailability and a high cost of production. In contrast, small-molecule compound-based fusion inhibitors are expected to have oral bioavailability and the advantage of low cost of production. This has sparked the discovery of a series of small-molecule inhibitors targeting HIV-1 gp41. For example, a series of N-substituted pyrrole derivatives, like NB-2 and NB-64, presents

* Corresponding authors.
E-mail addresses: shibojiang@fudan.edu.cn (S. Jiang), shmyf@hebau.edu.cn (F. Yu).
[1] These authors contributed equally to this work.

https://doi.org/10.1016/j.crmicr.2024.100260

Available online 9 July 2024

anti-HIV-1 infection activity by binding the hydrophobic pocket of gp41 and forming a salt bridge between the carboxyl and a positively charged residue Lys574 in gp41 (Jiang et al., 2004; Qiu et al., 2019; Teixeira et al., 2008). Additionally, a series of furan analogues, such as NB206, was reported to have low micromolar inhibitory activity against HIV-1 fusion by interacting with Lys574, Trp571, Gln577, and Arg579 in the gp41 NHR hydrophobic cavity (Katritzky et al., 2009). Trilobatin, as a strong natural sweetener, is a glycosylated dihydrochalcone that can suppress HIV-1 infection by interacting with the hydrophobic residues Leu559 and Ile564 located in the pocket of gp41 NHR (Yin et al., 2018). A phenylazo-naphthalene sulfonic acid derivative, ADS-J1, which we previously reported, also has broad-spectrum antiviral activity against HIV-1 infection by targeting the hydrophobic residues L568, V570, and W571 in the gp41 pocket (Armand-Ugon et al., 2005; Debnath et al., 1999; Jiang et al., 1999). Moreover, it can block fibril-mediated enhancement of HIV-1 infection (Xun et al., 2015). However, these fusion inhibitors all have some shortcomings like low druggability and low safety that call for further development, and the discovery of new compounds with effective anti-HIV activity and safety is worth researching.

Here, we report the development of HIV fusion inhibitor ADS-J21, which shares the same Y-shaped structure and the sulfonic acid as ADS-J1, but it has a lower molecular weight (689 Dalton *vs* 1176 Dalton) due to the removal of the redundancy group (Hu et al., 2023). Also, the safety was improved because ADS-J21 does not include the azo bond (Fig. 1) (Josephy and Allen-Vercoe, 2023). ADS-J21 exhibited HIV-1 inhibitory activity on both HIV-1 laboratory-adapted strains and primary isolates. Mechanistic studies have suggested that ADS-J21 effectively inhibits HIV-1 infection by targeting the conserved amino acids Lys35 (Lys574) and Trp32 (Trp571) within NHR of gp41. All results showed that ADS-J21 could serve as a lead compound for further optimization for improvement of its antiviral potency before further as a broad-spectrum antiviral agent.

2. Materials and methods

2.1. Cell lines, HIV-1 strains and Env expression vector

MT-2 cells, CEMx174 5.25M7 cells, 293T cells, U87.CD4.CCR5.CXCR4 cells, 183–12H-5C cells (expressing anti-p24 mAb), and H9/HIV-1_{IIIB} cells were obtained from the HIV Reagent Program. All the cells were cultured as previously described (Wang et al., 2009; Yu et al., 2012). HIV-1 wild-type or mutant Env expression vector and different HIV-1 laboratory-adapted strains, primary isolates, and T-20-resistant strains were also obtained from the HIV Reagent Program.

2.2. Inhibition of HIV-1 pseudovirus infection

2.2.1. Pseudovirus preparation

Wild-type and mutant HIV-1 pseudoviruses (PsVs) with Env were generated as described previously (Lu et al., 2012; Yu et al., 2012). Env expression plasmid with wild-type or mutant envelope glycoproteins and Env-deficient viral reporter vector (pNL4–3-Luc-R-E-) were cotransfected to 293T cells using Lipofectamine2000 (Thermo Fisher) for 48 h. Supernatants were centrifuged at 4000 rpm for 10 min, and filtrated by 0.45 μm filter. Then the supernatants were serially diluted and added to cell culture to infect U87.CD4.CXCR4.CCR5 cells for 24 h. Cell lysis was mixed with luciferase (Promega) and measured with the Infinite M1000 reader (Tecan). Wells producing relative luminescence units (RLU) 4 times the background were scored as positive, and the $TCID_{50}$ was calculated by the Spearman-Karber statistical method.

2.2.2. Single-cycle neutralization assay

The inhibitory activity of small-molecule compounds was tested on pseudotyped HIV-1 strains with different subtypes, and ADS-J1 was used as a control (Yu et al., 2012). Briefly, 50 μL of tested compounds at gradient concentrations were mixed with 50 μL of the pseudovirus supernatant at about 100 $TCID_{50}$. After incubation for 30 min, the mixtures were added to 1×10^4 cells/well U87.CD4.CXCR4.CCR5 cells at 37 °C for 2 days. The cells were lysed and measured for luciferase activity as described in 2.2.1.

2.3. Inhibitory activity of compounds against HIV-1 viruses

The inhibitory activity of ADS-J21 against different HIV-1 laboratory-adapted strains, primary isolates and T-20-resistant strains was tested as described previously (Jiang et al., 2004). Briefly, 50 μL of tested compounds with concentration gradient were incubated with 100 $TCID_{50}$ HIV-1 virons at 37 °C for 30 min, followed by the addition of target cells (1×10^4 cells/well of MT-2 cells or CEMx174 5.25M7 cells). After incubation at 37 °C for 24 h, the culture medium was replaced with 150 μL fresh culture medium with 10 % FBS (Gibco). After 72 h, p24 antigen was detected using the enzyme-linked immunosorbent assay (ELISA).

2.4. In vitro cytotoxicity assay of ADS-J21

The cytotoxicity of ADS-J21 and ADS-J1 in cells (MT-2, U87.CD4.

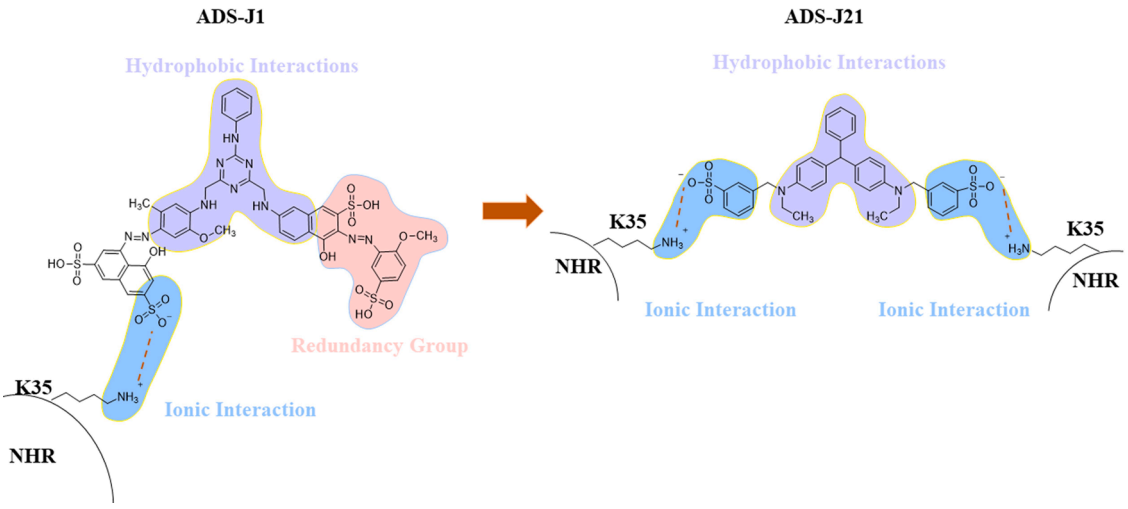

Fig. 1. Structure of ADS-J1 and ADS-J21. ADS-J1 was grouped into three parts, including hydrophobic interaction, ionic interaction and redundancy group. ADS-J21 was grouped into three parts, including hydrophobic interaction, and two ionic interactions.

CXCR4.CCR5 and CEMx174 5.25M7 cells) was tested using the CCK-8 kit (YEASEN). Briefly, 100 μL compounds at gradient concentrations were added to 100 μL of target cells (5×10^5 cells/mL). After incubation at 37 °C for 3 days, 50 μL of CCK-8 solution was added. After 4 h, the percentage of viable cells was quantified at 450 nm using the Infinite M1000 reader (Tecan). The 50 % cytotoxicity concentrations (CC_{50}) were calculated using CalcuSyn software (Chou and Talalay, 1984).

2.5. ELISA detection of p24 antigen levels

Wells of a plate (Costar) coated with HIV-IgG were blocked with 150 μL blocking buffer (2 % non-fat milk in PBS) at 37 °C for 1 h, followed washing three times with PBST (PBS containing 0.05 % Tween–20). Then 50 μL p24 supernatant from the inhibition of HIV-1 infection assay was incubated at 37 °C for 1 h and washed three times with PBST. 50 μL anti-p24 IgG (supernatant of NIH 183–12H-5C cells, 1:20 dilution in PBS) were then added to the plate and incubated at 37 °C for 1 h, washed three times with PBST. After that, 50 μL HRP-goat-anti-mouse IgG (1:2000 dilution in PBS) was added and incubated at 37 °C for 1 h, followed washing six times with PBST. Finally, 50 μL of substrates 3, 3′, 5, 5′-tetramethylbenzidine (TMB) solution were added and the reaction was stopped by adding 25 μL 0.5 M H_2SO_4. Optical density (OD) was read at 450 nm. The effective concentration for 50 % inhibition (IC_{50}) was calculated using the CalcuSyn software (Chou and Talalay, 1984).

2.6. HIV-1-mediated cell-cell fusion

HIV-1-mediated cell fusion was detected by dye transfer assay as described previously (Jiang et al., 1993; Lu et al., 2003). Briefly, $HIV\text{-}1_{IIIB}$-infected H9 cells were labelled with the fluorescent reagent Calcein AM for 30 min and washed with PBS three times. Then, in the presence or absence of graded concentration of ADS-J21 or ADS-J1, MT-2 cells were incubated with the labelled cells in wells of a 96-well plate at 37 °C for 2 h. The ratio of fused to unfused cells was counted under a fluorescence microscope (Nikon Eclipse, Japan). Three fields were calculated for per well. The inhibition rate of fusion was calculated using CalcuSyn software (Chou and Talalay, 1984).

2.7. Sandwich enzyme-linked immunosorbent assay (ELISA)

A sandwich ELISA was used to test the inhibitory activity of 6-HB formation of ADS-J21 as described previously Jiang et al., 1999; Wang et al., 2009(Jiang et al., 1999; Wang et al., 2009). A plate was coated with 50 μL of anti-N36/C34 IgG NY364 at 2 μg/mL in 0.1 M Tris buffer (pH 8.8) and incubated at 4 °C overnight and blocked with 2 % non-fat milk in PBS at 37 °C for 1 h. Peptide N36 (1 μM) was preincubated with ADS-J21 at a graded concentration at 37 °C for 30 min, followed adding C34-biotin (1 μM) at 37 °C for 30 min. For the control group, peptide N36 was preincubated with peptide C34 at 37 °C for 30 min, followed adding ADS-J21 at graded concentrations and washing. The mixture was added to coated plate (Costar) and incubated at 37 °C for 1 h. Then, 50 μL of mAb NC-1 IgG 2G8 at 1 μg/mL were added and incubated at 37 °C for 1 h, and then washed. Following that, HRP-goat-anti-mouse IgG (1:2000 dilution) was added and incubated at 37 °C for 1 h, and then washed. The TMB substrates were added sequentially. Absorbance at 450 nm was detected using an ELISA reader (Tecan, USA). Inhibitory activity was calculated as previously described (Jiang et al., 1999).

2.8. Native polyacrylamide gel electrophoresis (N-PAGE)

The formation of 6-HB was tested by N-PAGE as described previously (Liu et al., 2005). In brief, peptide N36 (40 μM) was preincubated with ADS-J21 at 37 °C for 30 min, and then peptide C34 (40 μM) was added and incubated with the mixture at 37 °C for 30 min. Following this, the samples were loaded (20 μL) into 18 % native-gels without boiling and run at 125 V constant voltage for 2 h. Finally, gels were stained with Coomassie blue and visualized with the FluorChem 8800 Imaging System (Alpha Innotech Corp., San Leandro, CA) (Liu et al., 2003).

2.9. Circular dichroism (CD) spectroscopy

CD spectroscopy was performed as described previously (Liu et al., 2005). Briefly, N36, C34, ADS-J21 were dissolved in PBS (pH 7.2). N36 was incubated with ADS-J21 or PBS at 37 °C for 30 min, followed by the addition of C34. In control, N36 was incubated with C34 at 37 °C for 30 min before adding ADS-J1, or PBS. After incubation at 37 °C for 30 min, the samples were cooled to room temperature. The spectra of each sample were acquired on a spectropolarimeter (Model J-715, Jasco Inc., Japan) at room temperature, using a 5.0 nm bandwidth, 0.1 nm resolution, 0.1 cm path length, 4.0 s response time, and 50 nm/min scanning speed. Spectra were then corrected by subtraction of a background corresponding to the solvent. $A[\theta]_{222}$ value of −33,000 deg cm^2 $dmol^{-1}$ was taken to correspond to 100 % α-helical content as described previously (Chan et al., 1998).

2.10. Molecular modeling

The Maestro software package was used to complete the flexible docking of ADS-J21 (Schrödinger Release 2024–2: Maestro, Schrödinger, LLC, New York, NY, 2024) and the top-scoring pose was shown by the software of PyMOL (http://pymol.sourceforge.net/). The gp41 was downloaded from the RCSB database (PDB Code: 2ZFC) and generated with the Protein prepration wizard in default parameters. ADS-J21 was generated via LigPrep and the most negative binding energy was chosen. A possible binding pocket around Lys35 and Trp32 was identified after Ligpre and SiteMap analysis. Then glide docking was performed, and the binding mode of ADS-J21 with three NHR region subunits was obtained.

2.11. Site-directed mutagenesis

The plasmid encoding HIV-1 SF162-Env was used to generate wild-type HIV-1 SF162 pseudovirus and HIV-1 SF162-Env mutants. Using the primers designed (“K35A-F: AACTCACAGTCTGGGGCATCGCGCAG CTCCAGGCAAGAGTCCT” and “W32A-F: CAGCATCTGTTGCAACTCA-CAGTCGCGGGCATCAAGCAGCTC”), a series of plasmids encoding HIV-1 SF162-Env mutants were prepared by polymerase chain reaction (PCR). After verifying the accuracy of the SF162-Env mutants by DNA sequencing, the pseudoviruses carrying the SF162-Env mutants were generated by transformation and amplification in 293T cells as described in 2.1.1. The inhibitory activity of ADS-J21 against HIV-1 SF162 infection by wild-type pseudotyped viruses and different HIV-1 SF162-Env mutants were tested using the single-cycle neutralization assay as described in 2.2.2. The effective concentration for 50 % inhibition (IC_{50}) was calculated using the CalcuSyn software (Chou and Talalay, 1984).

2.12. Analysis of synergy between ADS-J21 and FDA-approved antiviral drugs

Twenty-two FDA-approved antiviral drugs (FDA-ARDs) were individually tested in combination with ADS-J21 at an established molar ratio, which was optimized to give the greatest synergism over a range of serial dilutions. Inhibition data were analyzed for synergistic effects using the method of (Chou, 2006; Chou and Talalay, 1984). The analysis was conducted in a stepwise fashion by calculating IC_{50} values based on the dose-response curves of (i) single drugs (ADS-J21 and 22 ARDs) that were tested respectively and (ii) two drugs tested in combination (ADS-J21–22 ARDs) as described in 2.3 (Pan et al., 2009a,b). Then, the combination index (CI) was calculated using the median effect equation with the CalcuSyn program (kindly provided by T. C. Chou at Memorial Sloan-Kettering Cancer Center) to assess the synergistic effect of

combinations. A CI value ⟨1 indicates synergism. CI values were interpreted as follows: <0.1, very strong synergism; 0.1 – 0.3, strong synergism; 0.3 – 0.7, synergism; 0.7 – 0.85, moderate synergism; and 0.85 – 0.90, slight synergism. On the other hand, CI = 1 presents additive effects, and CI ⟩ 1 indicates antagonism (Chou and Talalay, 1984). Dose reduction was calculated by dividing the IC_{50} and IC_{90} values of ADS-J21 and ARDs when they were tested alone by that of the same drug tested in combination with other drugs.

3. Results

3.1. ADS-J21 presented highly inhibitory activity against different HIV-1 strains

To verify the anti-HIV-1 activity of ADS-J21, we determined its inhibitory activity against a series of pseudotyped HIV-1 laboratory-adapted and primary isolates, including CXCR4-tropic and CCR5-tropic strains. ADS-J21 showed inhibitory activity against laboratory-adapted HIV-1 CXCR4-tropic and CCR5-tropic strains, including subtypes A, B, C, D and recombinant strains C/D with IC_{50} from 0.40 to 5.81 μM (Fig. 2A-E and Table S1). ADS-J1 was used as a control with IC_{50} from 0.08 – 1.17 μM (Table S1). These data demonstrated that ADS-J21 exhibits broad-spectrum anti-HIV-1 pseudovirus potential, despite showing decreased anti-HIV-1 activity compared to that of ADS-J1.

We further assessed the inhibitory activity of ADS-J21 against HIV-1 laboratory-adapted strains and a panel of primary HIV-1 isolates *in vitro*, using ADS-J1 as controls. ADS-J21 showed inhibitory activity against HIV-1 laboratory-adapted CXCR4-tropic and CCR5-tropic (X4 and R5) strains, including HIV-1_{IIIB} with IC_{50} of 2.05 μM and HIV-1_{Bal} with IC_{50} of 2.53 μM (Fig. 2F, Table 1). Also, ADS-J21 could significantly inhibit infection by primary HIV-1 isolates of clades A to F (X4, R5, or X4R5) with IC_{50} values ranging from 1.29 – 10.05 μM (Table 1). More importantly, ADS-J21 presented effective inhibition of HIV infection by different T-20-resistant strains, including single-mutation and multi-mutation variants, and the IC_{50} values ranged from 2.41 – 6.79 μM (Table 2). Altogether, these results suggest that ADS-J21 has broad-spectrum anti-HIV-1 activity with low micromolar weight for all laboratory-adapted strains, primary HIV-1 strains and T-20-resistant strains.

Table 1
Inhibitory activity of ADS-J21 on infection by laboratory strains and primary HIV-1 isolates.[a]

Reagents	IC_{50} (μM)	
	ADS-J21	ADS-J1
Laboratory strains		
HIV_{IIIB}	2.05 ± 0.58	0.21 ± 0.04
HIV_{Bal}	2.53 ± 0.83	0.46 ± 0.24
Primary strains		
MN/H9 (84US_MNp) (A, X4)	3.16 ± 0.14	0.28 ± 0.05
KNH1088 (99KE_KNH1088) (A, R5)	4.01 ± 0.42	0.69 ± 0.17
KNH1144 (00KE_KNH1144) (A, R5)	3.39 ± 0.42	0.64 ± 0.35
KNH1207 (00KE_KNH1207) (A, R5)	4.69 ± 0.24	0.51 ± 0.01
BK132/GS 009 (90TH_BK132) (B, X4)	3.16 ± 0.45	0.99 ± 0.05
BZ167/GS 010 (89BZ_167) (B, X4)	4.01 ± 1.74	0.84 ± 0.20
US1/GS 004 (91US_1)(B,R5)	5.18 ± 0.17	1.09 ± 0.10
US4/GS 007 (91US_4) (B,R5)	6.77 ± 2.30	1.40 ± 0.17
SM145/GS 016 (89SM_145) (C, R5)	3.44 ± 0.16	1.00 ± 0.36
TZBD9/11 (01TZ_911) (C, R5)	1.29 ± 0.16	0.63 ± 0.05
93IN101(C, R5)	5.36 ± 0.29	1.76 ± 0.05
TZA68/125A(C, R5)	3.51 ± 0.72	0.92 ± 0.02
J32228M4(D, R5)	2.50 ± 0.71	0.28 ± 0.05
92UG024(D, X4)	1.60 ± 0.58	1.55 ± 0.69
CM235/GS 020 (90TH_CM235) (A/E, R5)	5.36 ± 0.29	0.63 ± 0.05
92TH009(A/E, R5)	10.05 ± 1.59	2.17 ± 1.65
93/BR/020(F, X4 and R5)	9.42 ± 2.65	2.95 ± 0.12

[a] Each sample was tested in triplicate and the experiment was repeated twice. The data from one representative experiment are presented as the mean ± standard deviation.

3.2. ADS-J21 had low cytotoxicity to HIV target cells in vitro

To evaluate the cytotoxicity of ADS-J21, its cytotoxicity on corresponding target cells (MT-2, U87.CD4.CXCR4.CCR5 and CEMx174 5.25M7 cells) was measured by CCK-8 assay. The CC_{50} was 189.55 μM for MT-2 cells, 259.09 μM for CEMx174 5.25M7 cells, and 435.91 μM for U87.CD4.R5.X4 cells (Table 3), suggesting that ADS-J21 exhibits low

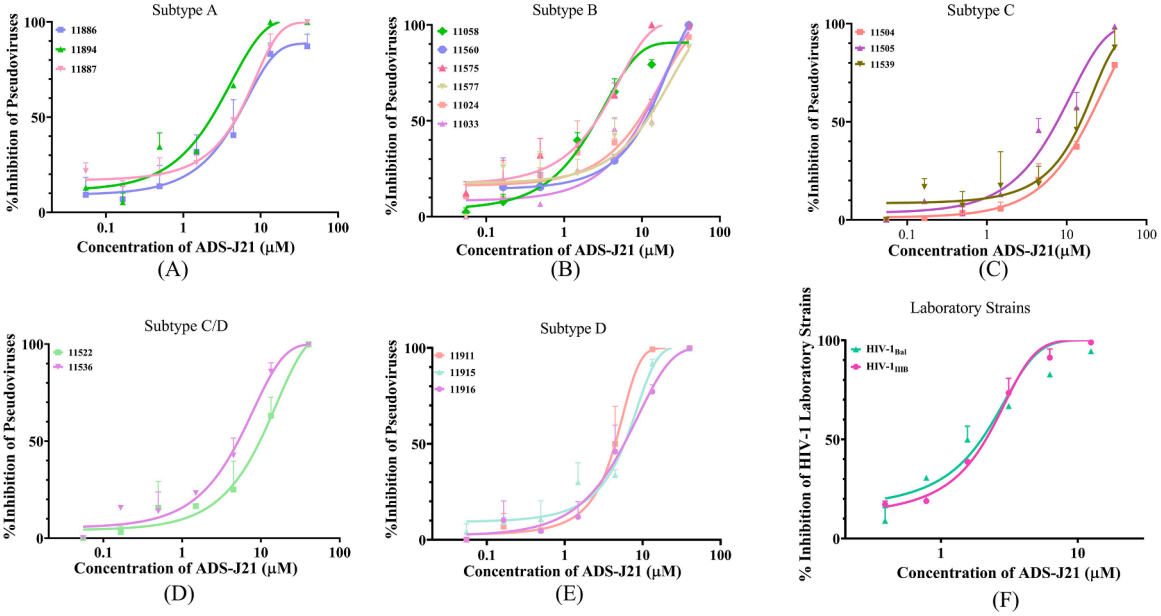

Fig. 2. Inhibitory activity of ADS-J21 on infection by primary HIV-1 strain pseudovirus. Briefly, ADS-J21 were mixed with 50 μL of the pseudovirus about 100 $TCID_{50}$ before the mixtures were added to the U87.CD4.CCR5.CXCR4 cells, then incubated at 37 °C for 30 min. After 2 days, the cells were lysed and measured for luciferase activity as described above. (**A**) subtype A, (**B**) subtype B, (**C**) subtype C, (**D**) subtype C/D, (**E**) subtype D. Single-cycle infection experiments were performed as described in Materials and Methods. (**F**) Laboratory strains. Each sample was tested in triplicate and the experiment was repeated twice. The data from one representative experiment are presented in mean ± standard deviation.

Table 2
Inhibitory activity of ADS-J21 on infection by T-20-resistant strains.[a]

T-20-resistant Strains	IC_{50} (μM)		
	ADS-J21	ADS-J1	T-20 (fold)[c]
NL4–3D36G[b]	6.79 ± 0.25	0.94 ± 0.01	0.04 ± 0.01
NL4–3(36 G)V38A/42D[b]	3.22 ± 0.53	0.85 ± 0.02	0.92 ± 0.18 (23)
NL4–3(36 G)V38A[b]	2.64 ± 0.01	0.93 ± 0.07	0.51 ± 0.01 (13)
NL4–3(36 G)N42T/43K[b]	2.41 ± 0.03	0.92 ± 0.04	0.56 ± 0.03 (14)
NL4–3(36 G)V38E/42S[b]	2.73 ± 0.06	1.98 ± 0.22	>2.00 (>50)
NL4–3(36 G)V38A/42T[b]	4.11 ± 0.48	1.26 ± 0.16	1.46 ± 0.38 (37)

[a] Each sample was tested in triplicate and the experiment was repeated twice. The data from one representative experiment are presented as the mean ± standard deviation.
[b] NL4–3D36G is a T20-sensitive strain, which was the parent strain used for the generation of T20-resistant mutants, including NL4–3(36G)V38A, NL4–3(36G)V38A/42D, NL4–3(36G)V38A/42T, NL4–3(36G)V38E/42S, NL4–3(36G)N42T/43K.
[c] Fold of resistance relative to the T20-sensitive strain, NL4–3D36G.

Table 3
In vitro cytotoxicity of ADS-J21 and ADS-J1.[a]

Cell type	CC_{50} (μM)	
	ADS-J21	ADS-J1
MT-2	189.55 ± 14.42	263.99 ± 29.33
CEMx174 5.25M7	259.09 ± 44.20	449.93 ± 33.00
U87.CD4.R5.X4	435.91 ± 32.57	514.91 ± 6.00

[a] Each sample was tested in triplicate and the experiment was repeated twice. The data from one representative experiment are presented as the mean ± standard deviation.

cytotoxicity on all tested cells. Importantly, the median CC_{50} on all tested cells for ADS-J21 is 100-fold higher than the median IC_{50} on all tested HIV strains, suggesting that ADS-J21 can effectively inhibit a broad spectrum of HIV-1 infection at concentrations far below those of cell cytotoxicity.

3.3. ADS-J21 can inhibit HIV-1-mediated cell-cell fusion

In addition to virus-cell fusion of HIV-1, HIV-1-mediated cell-cell fusion is another important pathway for HIV-1 infection. Therefore, we further evaluated the cell-cell fusion inhibitory activity of ADS-J21 by stably transfecting H9/HIV-1_{IIIB} cells and MT-2 cells (Jiang et al., 2000). The IC_{50} of ADS-J21 against cell-cell fusion inhibitory activity is 12.69 μM (the IC_{50} values of ADS-J1 and T-20 are 5.84 μM and 10.7 nM, respectively) (Fig. 3 and Table S2), suggesting that ADS-J21 is also an effective cell-cell fusion inhibitor.

3.4. ADS-J21 inhibited the formation of gp41 core between NHR and CHR peptides

The formation of 6-HB between NHR trimer and CHR trimer is an important step in the early process of membrane fusion when HIV-1 infects target cells (Chan et al., 1997; Chan and Kim, 1998; Debnath et al., 1999; Jiang et al., 2004; Lu et al., 1995; Pancera et al., 2010; Weissenhorn et al., 1997; Yu et al., 2013). Previous data showed that ADS-J1 can suppress HIV-1 entry into target cells by restraining the formation of 6-HB (Armand-Ugon et al., 2005; Gonzalez-Ortega et al., 2010; Yu et al., 2014). Therefore, we hypothesized that ADS-J21, as a derivative of ADS-J1 with a similar Y-shaped structure, could also block 6-HB fusion core formation (Debnath et al., 1999; Jiang et al., 1999; Yu et al., 2014). Thus, we investigated the antiviral mechanism of ADS-J21 by using a mature model of gp41 core including N36 (an NHR-derived peptide) and C34 (a CHR-derived peptide) to simulate the formation of gp41 6-HB *in vitro* (Liu et al., 2003).

Based on the ELISA assay, Fig. 4A shows that ADS-J21 could inhibit 6-HB core formation with IC_{50} of 16.26 μM when it was incubated with N36 before the addition of C34. However, when ADS-J21 was added after the binding of N36 and C34, it was almost not inhibited for the formation of 6-HB at a concentration less than 100 μM. This result suggested that ADS-J21 can block gp41 6-HB core formation by interacting with gp41 NHR, but has no inhibition after gp41 6-HB core formation.

Based on the N-PAGE assay in Fig. 4B, the C34 peptide showed a single band at the lower position (lane 1), while the mixture of C34 and N36 peptides appeared as an additional specific band at the upper position (lane 2–3). The intensities of the specific bands at the upper position decreased after incubating ADS-J21 with N36 before the addition of C34 peptides (lane 4). However, when N36 was incubated with C34 before ADS-J21 was added, ADS-J21 showed no inhibitory activity (lane 5). The negative control AZT (lanes 6–7) and the positive control ADS-J1 (lanes 8–9) showed similar properties. Therefore, we further confirmed

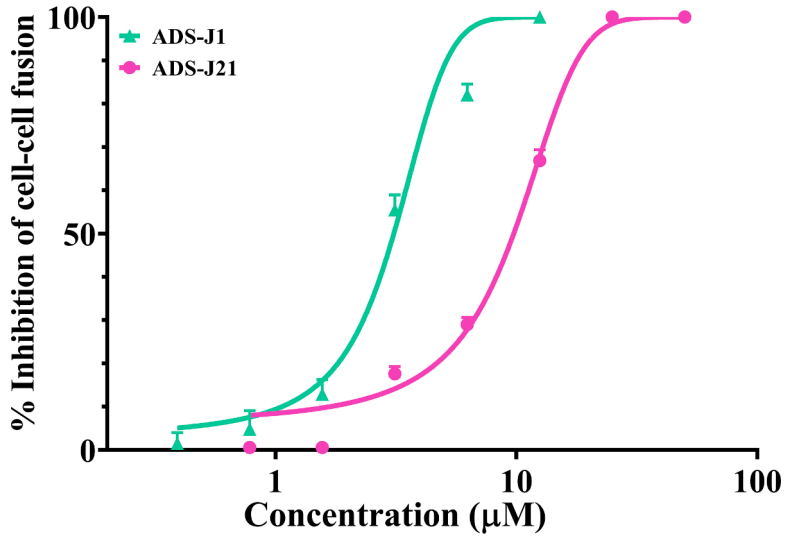

Fig. 3. ADS-J21 can inhibit HIV-1-mediated cell-cell fusion. MT-2 cells were incubated with H9/HIV-1_{IIIB} labelled with Calcein AM for 30 min together with a gradient concentration of ADS-J21. Compared with the group of (H9/HIV-1_{IIIB}+MT-2), 50 μM ADS-J21 can completely inhibit HIV-1-mediated cell-cell fusion. ADS-J1 is a positive control. Each sample was tested in triplicate and the experiment was repeated twice. The data from one representative experiment were presented in means ± standard deviation.

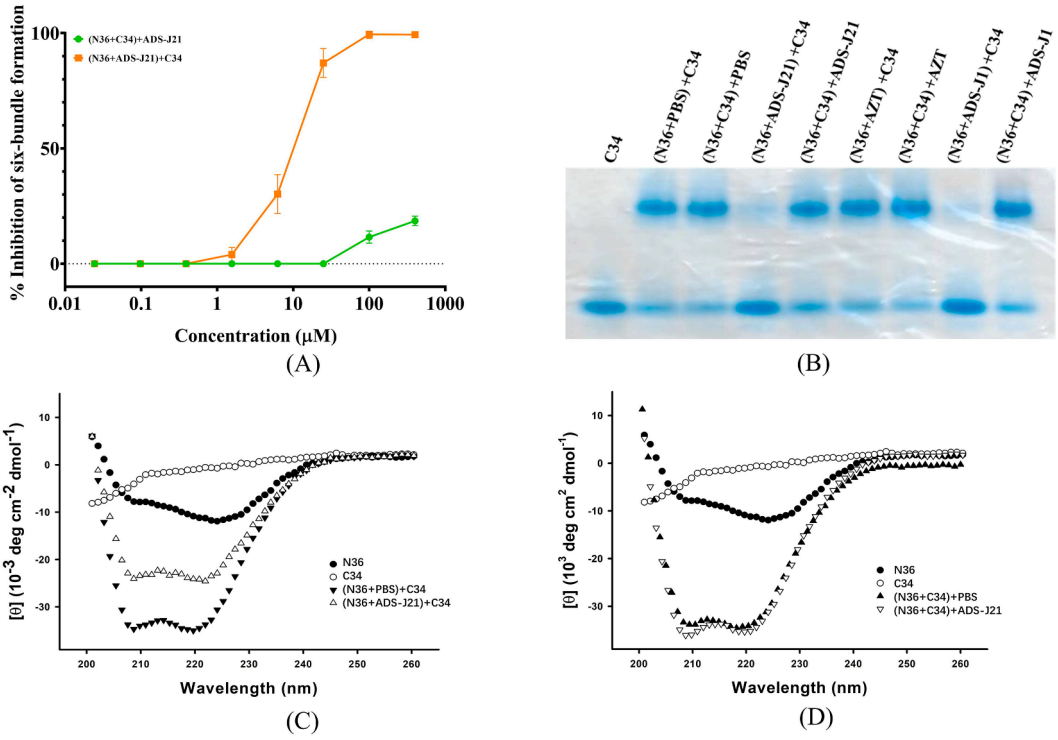

Fig. 4. ADS-J21 can block 6-HB core formation by interfering with the interaction between gp41 NHR and CHR. (**A**) Using ELISA, ADS-J21 was incubated with the N36 peptide before the addition of the C34 peptide, and ADS-J21 could inhibit 6-HB core formation in a dose-dependent manner with an IC_{50} value of 16.25 μM. (**B**) Using N-PAGE, the C34 (40 μM) peptide showed a single band at the lower position (lane 1), while the mixture of C34 and N36 (40 μM) peptides appeared as an additional specific band at the upper position (lane 2–3). Intensities of the specific bands at the upper position decreased after incubating ADS-J21 with N36 before the addition of C34 peptides (lane 4). However, when N36 was incubated with C34 first and then ADS-J21 was added, ADS-J21 showed no inhibitory activity (lane 5). Here, the negative control, AZT (lane 6–7), and ADS-J1 (lane 8–9) showed similar properties. Using CD, compared with the addition of ADS-J21 before C34 (**C**), ADS-J21 could not alter the α-helical structure of the preformed N36-C34 complex (**D**).

that ADS-J21 interacts with gp41 NHR to block 6-HB core formation, thus possessing anti-HIV-1 infection inhibitory, whereas it fails to act after 6-HB core formation. Hence, the results of the N-PAGE assay further verify that ADS-J21 acts as a 6-HB blocker.

Subsequently, the effect of ADS-J21 on the secondary structure of 6-HB was investigated by circular dichroism (Lu et al., 1995). Previous research demonstrated that individual NHR peptides or CHR peptides have a random coil structure in aqueous solution, but that the mixture of NHR and CHR peptides showed a typical α-helical conformation (Lu et al., 1995). In Fig. 4C, the α-helicity between the N36 and C34 peptides was completely inhibited by incubating ADS-J21 with N36 before the addition of C34 peptides. In contrast, ADS-J21 was unable to alter the α-helical structure of the preformed N36-C34 complex (Fig. 4D), and the results between positive control ADS-J1 and ADS-J21 by CD spectroscopy were completely consistent. Taken together, these results indicated that ADS-J21 could block the formation of HIV-1 gp41 core between NHR and CHR peptides by significantly interfering with their interaction to form α-helical content.

3.5. *Lys35 and Trp32 were key binding residues used by ADS-J21 to inhibit HIV-1 infection*

The binding style of ADS-J21 with HIV-1 gp41 NHR (PDB Code: 2ZFC) was predicted by using Schrödinger software. As shown in Fig. 5, the sulfonic acid moiety of the ADS-J21 was extended to the hydrophobic pocket formed by Ala29, Gly33, Gln38, Leu30, Val34, Val31, and Lys35. The two sulfonic acid groups in the benzene ring form two arms that tightly grab one chain of NHR like a binder clip through hydrogen

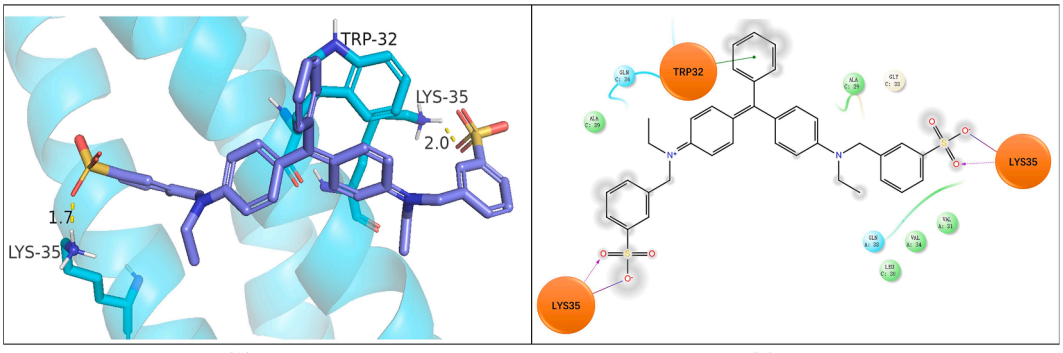

Fig. 5. Possible binding mode of ADS-J21 with HIV-1. (**A**) Proposed binding mode of ADS-J21 (purple) with HIV-1 gp41 NHR (PDB code 2ZFC). (**B**) 2D mode of ADS-J21 with HIV-1 gp41 NHR.

bond formation by the interaction of electronegative sulfonic acid with Lys35 (Lys574). In parallel, the benzene ring of ADS-J21 formed a π-π stacking interaction with Trp32 to help ADS-J21 grab NHR stably.

To verify the docking result, we designed single site-directed HIV-1 SF162-Env mutants K35A and W32A, both of which rendered HIV-1 SF162 pseudovirus highly resistant to ADS-J21 (Fig. 6 and Table S3). The inhibitory activity of ADS-J21 on W32A and K35A mutants reduced 6.9-fold and >19.3-fold than that for SF162-WT pseudovirus, respectively (Fig. 6 and Table S3). K35 in N36 PFD interact with D632 in C34 PBD to form a salt bridge and promote the formation of 6-HB (He et al., 2008). These results suggest that W32 and K35 are key residues for the binding of ADS-J21 with gp41 NHR and further confirm that the electronegative sulfonic acid and benzene ring are the key pharmacophores of ADS-J21.

3.6. Analysis of synergy between ADS-J21 and FDA-approved ARDs

The rapid emergence of drug-resistant variants in ARD-treated patients is one of the major causes of failed ARD therapy (Rambaut et al., 2004). The combination of multiple anti-HIV-1 drugs named highly active antiretroviral therapy (HRRT) is an effective therapy for reducing the emergence of drug-resistant variants. Hence, we tested the potential synergistic effect between ADS-J21 and 22 ARDs on the inhibition of HIV-1_{IIIB} infection on MT-2 cells as previously described (Liu et al., 2005; Pan et al., 2009a,b). The combination of ADS-J21 with 11 of 22 ARDs (Stavudine, Zalcitabine, Tenofovir disoproxil fumarate, Delavirdine, Etravirine, Efavirenz, Dapivirine, Ritonavir, Darunavir, Nelfinavir, Enfuvirtide) exhibited a synergistic effect in inhibiting infection by HIV-1_{IIIB} with an increase of potency ranging from 2.9-fold to 72.6-fold (Table S4 and Fig. 7).

The ARD enfuvirtide (T-20) exhibited a significant synergistic effect among the 11 tested compounds, resulting in a remarkable 72.6-fold increase in IC_{50}, whereas Delavirdine had the lowest synergistic effect with an IC_{50} increase of 2.9-fold. As the first-generation FIs, the T-20 has shortcomings of high cost and use of injection. However, the combined utilization of ADS-J21 with enfuvirtide may reduce the dosage and frequency of drug use.

3.7. Analysis of physicochemical properties and drug-likeness properties of ADS-J21

Next, we further evaluated the physicochemical properties and drug-likeness of ADS-J1 and ADS-J21 by SwissADME (http://www.swissadme.ch/). As shown in Figure S1 and Table S5, although ADS-J1 and ADS-J21 both do not meet Lipinski's rule and drug-likeness rules, ADS-J21 presented a better physicochemical and drug-likeness properties than ADS-J1. In addition, ADS-J21 showed better bioavailability scores than ADS-J1 (0.56 VS 0.11). All these data indicate that ADS-J21 could be further investigated as an anti-HIV drug.

4. Discussion

In this study, we discovered a new compound ADS-J21, which has a Y-shaped structure similar to that of ADS-J1. The results from *in vitro* assays revealed that ADS-J21 has effective antiviral activity against infection by a broad-spectrum of HIV-1 laboratory strains and primary isolates, although its potency is not as high as that of ADS-J1. Mechanism studies demonstrate that ADS-J21 blocks the gp41 6-HB formation by targeting the conserved amino acids Lys35 and Trp32 in the NHR pocket of gp41. In addition, the combinations of ADS-J21 with 11 out of 22 ARDs tested show synergistic anti-HIV-1 effect with about 2.9 to 72.6-fold increased potency. Moreover, the prediction of physicochemical properties and drug-likeness by SwissADME shows that ADS-J21 has better druggability than ADS-J1.

ADS-J21 was designed and synthesized based on the chemical structure of ADS-J1. Structurally, ADS-J21 includes a triphenylmethane skeleton and two sulfonic acids. These groups are common in some antiviral compounds (Chen et al., 2009; Hu et al., 2023; Radi et al., 2022). The benzene ring was extended and grafted for further optimization. ADS-J21 has a lower molecular weight (689 Da) than that of ADS-J1 (1176 Da). The chemical structure of ADS-J1 is complicated, including one triazine, two naphthalene rings, two azos groups, three benzene rings and four sulfonic acids (Hu et al., 2023). Besides, its azo bonds carry the risk of reductive metabolism toxicity, which can be metabolized into toxic aromatic amines (Josephy and Allen-Vercoe, 2023). Although ADS-J21 has a similar Y-shaped structure as ADS-J1,

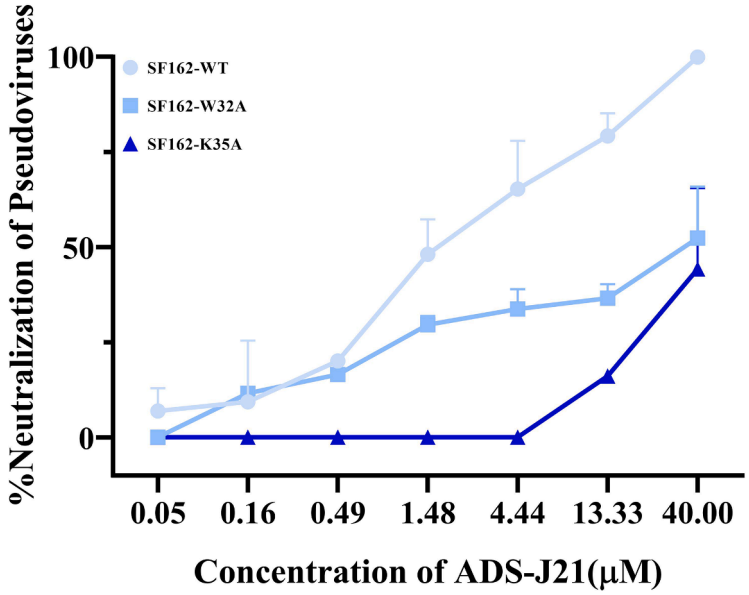

Fig. 6. Inhibitory activity of ADS-J21 on infection by SF162-WT, SF162-K35A and SF162-W32A pseudoviruses. Each sample was tested in triplicate and the experiment was repeated twice. The data from one representative experiment are presented as the mean ± standard deviation.

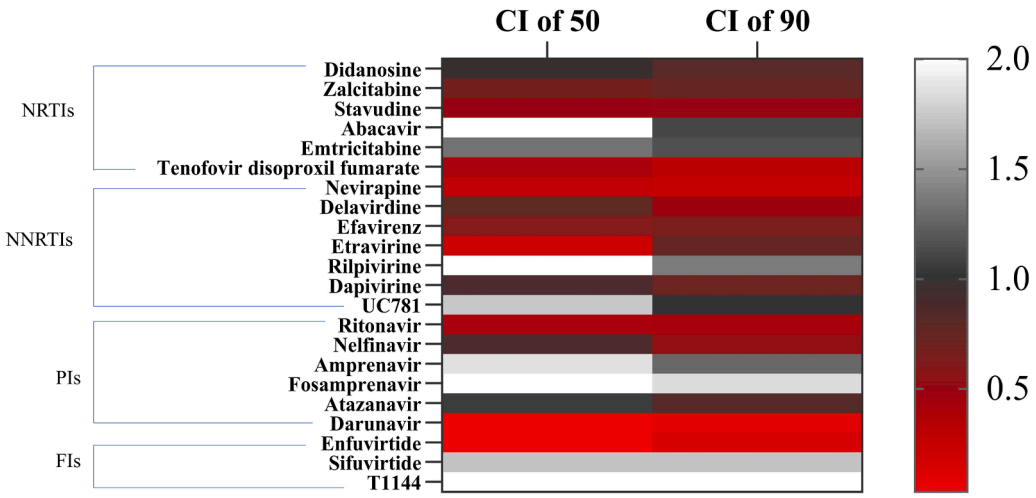

Fig. 7. CI and dose reduction in inhibition of infection by laboratory-adapted and primary HIV-1 strains by combining ADS-J21 and 11 ARDs. Combination index (CI) value <1 indicates synergism. Specifically, CI values <0.1, 0.1 - 0.3, 0.3 - 0.7, 0.7 - 0.85, and 0.85 – 0.90, mean very strong synergism, strong synergism; synergism; moderate synergism, and slight synergism, respectively. The red lane represents high synergistic efficacy, the gray lane low synergistic efficacy, and the white lane strong antagonistic action. Nucleoside Reverse Transcriptase Inhibitors (NRTIs), Nonnucleoside Reverse Transcriptase Inhibitors (NNRTIs), Protease Inhibitors (PIs), and Fusion Inhibitors (FIs).

ADS-J21 has a simpler chemical structure and contains no azo bonds, thus being easier for structure optimization and SAR analysis. The bioavailability predicted by SwissADME has shown that ADS-J21 presents better drug-likeness properties and superior bioavailability scores than ADS-J1 (0.56 *VS* 0.11) (Figure S1 and Table S5), indicating that ADS-J21 may have better safety *in vivo*. These findings suggest that ADS-J21 has better drugability and potential for optimation than ADS-J1.

In conclusion, ADS-J21 has a lower molecular weight, simpler structure and better druggability than ADS-J1, making it a better lead compound for further optimization. Its *in vitro* antiviral activity, mechanism of action, and synergistic effect when combined with other ARDs tested highlight its potential as an effective anti-HIV-1 agent for further optimization and development as a novel antiviral drug for treatment or prevention of HIV-1 infection in the future.

Funding

This work was supported by grants from the National Natural Science Foundation of China (81501735), the Natural Science Foundation of Hebei Province (H2021204001), Hebei Province's Program for Talents Returning from Studying Overseas (CN201707), the Program for Youth Talent of Higher Learning Institutions of Hebei Province (BJ2018045), Science Research Project of Hebei Education Department (QN2022010), and Baoding Science and Technology Plan Project (2272P006 and 2172P008). Shanghai Municipal Science and Technology Major Project (ZD2021CY001 to S.J.)

CRediT author statement

F.Y. and S.J. conceived the idea and supervised the project; R.L., D. D., S.H., Y.W., J.W., Z.Y., S.Z., J.X., Y.L., and P.L. performed the experiments; R.L. D.D., C.W and drafted the manuscript; F.Y. and S.J. revised the manuscript. All authors have read and agreed to the published version of the manuscript.

Declaration of competing interest

The authors declare that they have no known competing financial interests or personal relationships that could have appeared to influence the work reported in this paper.

Data availability

Data will be made available on request.

Supplementary materials

Supplementary material associated with this article can be found, in the online version, at doi:10.1016/j.crmicr.2024.100260.

References

Armand-Ugon, M., Clotet-Codina, I., Tintori, C., Manetti, F., Clotet, B., Botta, M., Este, J. A., 2005. The anti-HIV activity of ADS-J1 targets the HIV-1 gp120. Virology. 343, 141–149. https://doi.org/10.1016/j.virol.2005.08.007.

Berger, E.A., 1997. HIV entry and tropism: the chemokine receptor connection. AIDS 11 (Suppl A), S3–16.

Bernstein, H.B., Tucker, S.P., Kar, S.R., Mcpherson, S.A., Mcpherson, D.T., Dubay, J.W., Lebowitz, J., Compans, R.W., Hunter, E., 1995. Oligomerization of the hydrophobic heptad repeat of Gp41. J. Virol. 69, 2745–2750. https://doi.org/10.1128/JVI.69.5.2745-2750.1995.

Capon, D.J., Ward, R.H., 1991. The CD4-gp120 interaction and AIDS pathogenesis. Annu. Rev. Immunol. 9, 649–678. https://doi.org/10.1146/annurev.iy.09.040191.003245.

Chan, D.C., Chutkowski, C.T., Kim, P.S., 1998. Evidence that a prominent cavity in the coiled coil of HIV type 1 gp41 is an attractive drug target. P Natl Acad Sci Usa. 95, 15613–15617. https://doi.org/10.1073/pnas.95.26.15613.

Chan, D.C., Fass, D., Berger, J.M., Kim, P.S., 1997. Core structure of gp41 from the HIV envelope glycoprotein. Cell 89, 263–273. https://doi.org/10.1016/s0092-8674(00)80205-6.

Chan, D.C., Kim, P.S., 1998. HIV entry and its inhibition. Cell 93, 681–684. https://doi.org/10.1016/s0092-8674(00)81430-0.

Chen, C.-S., Chiou, C.-T., Chen, G.S., Chen, S.-C., Hu, C.-Y., Chi, W.-K., Chu, Y.-D., Hwang, L.-H., Chen, P.-J., Chen, D.-S., Liaw, S.-H., Chern, J.-W., 2009. Structure-based discovery of triphenylmethane derivatives as inhibitors of hepatitis C virus helicase. J. Med. Chem. 52, 2716–2723. https://doi.org/10.1021/jm8011905.

Chou, T.C., 2006. Theoretical basis, experimental design, and computerized simulation of synergism and antagonism in drug combination studies. Pharmacol. Rev. 583, 621–681. https://doi.org/10.1124/pr.58.3.10.

Chou, T.C., Talalay, P., 1984. Quantitative analysis of dose-effect relationships: the combined effects of multiple drugs or enzyme inhibitors. Adv. Enzyme Regul. 22, 27–55. https://doi.org/10.1016/0065-2571(84)90007-4.

Debnath, A.K., Radigan, L., Jiang, S., 1999. Structure-based identification of small molecule antiviral compounds targeted to the gp41 core structure of the human immunodeficiency virus type 1. J. Med. Chem. 42, 3203–3209. https://doi.org/10.1021/jm990154t.

Dimitrov, D.S., 1997. How do viruses enter cells? The HIV coreceptors teach us a lesson of complexity. Cell 91, 721–730. https://doi.org/10.1016/S0092-8674(00)80460-2.

Gonzalez-Ortega, E., Mena, M.P., Permanyer, M., Ballana, E., Clotet, B., Este, J.A., 2010. ADS-J1 inhibits HIV-1 entry by interacting with gp120 and does not block fusion-

active gp41 core formation. Antimicrob Agents Ch 54, 4487–4492. https://doi.org/10.1128/AAC.00359-10.

He, Y., Xiao, Y., Song, H., Liang, Q., Ju, D., Chen, X., Lu, H., Jing, W., Jiang, S., Zhang, L., 2008. Design and evaluation of sifuvirtide, a novel HIV-1 fusion inhibitor. J. Biol. Chem. 283, 11126–11134. https://doi.org/10.1074/jbc.M800200200.

Hu, L., Jia, H., Zhang, J., da Silva-Júnior, E.F., Liu, C., Liu, X., Zhan, P., 2023. Sulfonic acid: key drug design elements with potent, broad-ranging pharmacological activities. Future Med. Chem. 15, 2029–2032. https://doi.org/10.4155/fmc-2023-0257.

Huang, C.C., Tang, M., Zhang, M.Y., Majeed, S., Montabana, E., Stanfield, R.L., Dimitrov, D.S., Korber, B., Sodroski, J., Wilson, I.A., Wyatt, R., Kwong, 2005. Structure of a V3-containing HIV-1 gp120 core. Science 310, 1025–1028. https://doi.org/10.1126/science.1118398.

Jiang, S.B., Lin, K., Strick, N., Neurath, A.R., 1993. HIV-1 inhibition by a peptide. Nature 365, 113. https://doi.org/10.1038/365113a0.

Jiang, S.B., Lu, H., Liu, S.W., Zhao, Q., He, Y.X., Debnath, A.K., 2004. N-substituted pyrrole derivatives as novel human immunodeficiency virus type 1 entry inhibitors that interfere with the gp41 six-helix bundle formation and block virus fusion. Antimicrob Agents Ch 48, 4349–4359. https://doi.org/10.1128/Aac.48.11.4349-4359.2004.

Jiang, S., Radigan, L., Zhang, L., 2000. Convenient cell fusion assay for rapid screening for HIV entry inhibitors. Biomedical optics 392, 212–219. https://doi.org/10.1117/12.380514.

Jiang, S.B., Lin, K., Zhang, L., Debnath, A.K., 1999. A screening assay for antiviral compounds targeted to the HIV-1 gp41 core structure using a conformation-specific monoclonal antibody. J. Virol. Methods 80, 85–96. https://doi.org/10.1016/S0166-0934(99)00041-5.

Josephy, P.D., Allen-Vercoe, E., 2023. Reductive metabolism of azo dyes and drugs: toxicological implications. Food Chem. Toxicol. 178, 113932 https://doi.org/10.1016/j.fct.2023.113932.

Katritzky, A.R., Tala, S.R., Lu, H., Vakulenko, A.V., Chen, Q.Y., Sivapackiam, J., Pandya, K., Jiang, S., Debnath, A.K., 2009. Design, synthesis, and structure-activity relationship of a novel series of 2-aryl 5-(4-oxo-3-phenethyl-2-thioxothiazolidinylidenemethyl)furans as HIV-1 entry inhibitors. J. Med. Chem. 52, 7631–7639. https://doi.org/10.1021/jm900450n.

Kwon, Y.D., Finzi, A., Wu, X., Dogo-Isonagie, C., Lee, L.K., Moore, L.R., Schmidt, S.D., Stuckey, J., Yang, Y., Zhou, T., Zhu, J., Vicic, D.A., Debnath, A.K., Shapiro, L., Bewley, C.A., Mascola, J.R., Sodroski, J.G., Kwong, 2012. Unliganded HIV-1 gp120 core structures assume the CD4-bound conformation with regulation by quaternary interactions and variable loops. Proc. Natl. Acad. Sci. U. S. A. 109, 5663–5668. https://doi.org/10.1073/pnas.1112391109.

Leal, L., Guardo, A.C., Bedoya, L.M., Rodriguez de Miguel, C., Climent, N., Rovira, C., Beltran, M., Llach, J., Alcami, J., Kashuba, A.D.M., Gatell, J.M., Plana, M., Garcia, F., 2023. Pharmacokinetics, the immunological impact, and the effect on HIV ex-vivo infectivity of maraviroc, raltegravir, and lopinavir in men who have sex with men using postexposure prophylaxis. AIDS Res. Hum. Retroviruses 39, 211–221. https://doi.org/10.1089/AID.2021.0232.

Liu, S., Lu, H., Niu, J., Xu, Y., Wu, S., Jiang, S., 2005. Different from the HIV fusion inhibitor C34, the anti-HIV drug Fuzeon (T-20) inhibits HIV-1 entry by targeting multiple sites in gp41 and gp120. J. Biol. Chem. 280, 11259–11273. https://doi.org/10.1074/jbc.M411141200.

Liu, S., Zhao, Q., Jiang, S., 2003. Determination of the HIV-1 gp41 fusogenic core conformation modeled by synthetic peptides: applicable for identification of HIV-1 fusion inhibitors. Peptides. 24, 1303–1313. https://doi.org/10.1016/j.peptides.2003.07.013.

Lu, H., Zhao, Q., Xu, Z., Jiang, S., 2003. Automatic quantitation of HIV-1 mediated cell-to-cell fusion with a digital image analysis system (DIAS): application for rapid screening of HIV-1 fusion inhibitors. J. Virol. Methods 107, 155–161. https://doi.org/10.1016/s0166-0934(02)00213-6.

Lu, L., Tong, P., Yu, X., Pan, C., Zou, P., Chen, Y.H., Jiang, S., 2012. HIV-1 variants with a single-point mutation in the gp41 pocket region exhibiting different susceptibility to HIV fusion inhibitors with pocket- or membrane-binding domain. Biochim. Biophys. Acta 1818, 2950–2957. https://doi.org/10.1016/j.bbamem.2012.07.020.

Lu, M., Blacklow, S.C., Kim, P.S., 1995. A trimeric structural domain of the HIV-1 transmembrane glycoprotein. Nat. Struct. Biol. 2, 1075–1082. https://doi.org/10.1038/nsb1295-1075.

Pan, C., Cai, L., Lu, H., Qi, Z., Jiang, S., 2009a. Combinations of the first and next generations of human immunodeficiency virus (HIV) fusion inhibitors exhibit a highly potent synergistic effect against enfuvirtide- sensitive and -resistant HIV type 1 strains. J. Virol. 83, 7862–7872. https://doi.org/10.1128/JVI.00168-09.

Pan, C., Lu, H., Qi, Z., Jiang, S., 2009b. Synergistic efficacy of combination of enfuvirtide and sifuvirtide, the first- and next-generation HIV-fusion inhibitors. AIDS 23, 639–641. https://doi.org/10.1097/QAD.0b013e328325a4cd.

Pancera, M., Majeed, S., Ban, Y.E.A., Chen, L., Huang, C.C., Kong, L., Kwon, Y.D., Stuckey, J., Zhou, T.Q., Robinson, J.E., Schief, W.R., Sodroski, J., Wyatt, R., Kwong, P.D., 2010. Structure of HIV-1 gp120 with gp41-interactive region reveals layered envelope architecture and basis of conformational mobility. P Natl Acad Sci Usa. 107, 1166–1171. https://doi.org/10.1073/pnas.0911004107.

Poumbourios, P., Wilson, K.A., Center, R.J., El Ahmar, W., Kemp, B.E., 1997. Human immunodeficiency virus type 1 envelope glycoprotein oligomerization requires the gp41 amphipathic alpha-helical/leucine zipper-like sequence. J. Virol. 71, 2041–2049. https://doi.org/10.1128/JVI.71.3.2041-2049.1997.

Qiu, J., Liang, T., Wu, J., Yu, F., He, X., Tian, Y., Xie, L., Jiang, S., Liu, S., Li, L., 2019. N-Substituted pyrrole derivative 12m inhibits HIV-1 entry by targeting Gp41 of HIV-1 envelope glycoprotein. Front. Pharmacol. 10, 859. https://doi.org/10.3389/fphar.2019.00859.

Radi, R., Huang, C., Elsey, J., Jung, Y.H., Corces, V.G., Arbiser, J.L., 2022. Indolium 1 exerts activity against vemurafenib-resistant melanoma in vivo. Antioxidants. (Basel) 11, 798. https://doi.org/10.3390/antiox11050798.

Rambaut, A., Posada, D., Crandall, K.A., Holmes, E.C., 2004. The causes and consequences of HIV evolution. Nat. Rev. Genet. 5, 52–61. https://doi.org/10.1038/nrg1246.

Teixeira, C., Barbault, F., Rebehmed, J., Liu, K., Xie, L., Lu, H., Jiang, S.B., Fan, B.T., Maurel, F., 2008. Molecular modeling studies of N-substituted pyrrole derivatives - Potential HIV-1 gp41 inhibitors. Bioorg. Med. Chem. 16, 3039–3048. https://doi.org/10.1016/j.bmc.2007.12.034.

Wang, H., Qi, Z., Guo, A., Mao, Q., Lu, H., An, X., Xia, C., Li, X., Debnath, A.K., Wu, S., Liu, S., Jiang, S., 2009. ADS-J1 inhibits human immunodeficiency virus type 1 entry by interacting with the gp41 pocket region and blocking fusion-active gp41 core formation. Antimicrob Agents Ch 53, 4987–4998. https://doi.org/10.1128/AAC.00670-09.

Weissenhorn, W., Dessen, A., Harrison, S.C., Skehel, J.J., Wiley, D.C., 1997. Atomic structure of the ectodomain from HIV-1 gp41. Nature 387, 426–430. https://doi.org/10.1038/387426a0.

Xun, T., Li, W., Chen, J., Yu, F., Xu, W., Wang, Q., Yu, R., Li, X., Zhou, X., Lu, L., Jiang, S., Li, L., Tan, S., Liu, S., 2015. ADS-J1 inhibits semen-derived amyloid fibril formation and blocks fibril-mediated enhancement of HIV-1 infection. Antimicrob Agents Ch 59, 5123–5134. https://doi.org/10.1128/AAC.00385-15.

Yin, S., Zhang, X., Lai, F., Liang, T., Wen, J., Lin, W., Qiu, J., Liu, S., Li, L., 2018. Trilobatin as an HIV-1 entry inhibitor targeting the HIV-1 gp41 envelope. FEBS Lett. 592, 2361–2377. https://doi.org/10.1002/1873-3468.13113.

Yu, F., Lu, L., Du, L., Zhu, X., Debnath, A.K., Jiang, S., 2013. Approaches for identification of HIV-1 entry inhibitors targeting gp41 pocket. Viruses. 51, 127–149. https://doi.org/10.3390/v5010127.

Yu, F., Lu, L., Liu, Q., Yu, X., Wang, L., He, E., Zou, P., Du, L., Sanders, R.W., Liu, S., Jiang, S., 2014. ADS-J1 inhibits HIV-1 infection and membrane fusion by targeting the highly conserved pocket in the gp41 NHR-trimer. Biochim. Biophys. Acta 1838, 1296–1305. https://doi.org/10.1016/j.bbamem.2013.12.022.

Yu, X., Lu, L., Cai, L., Tong, P., Tan, S., Zou, P., Meng, F., Chen, Y.H., Jiang, S., 2012. Mutations of Gln64 in the HIV-1 gp41 N-terminal heptad repeat render viruses resistant to peptide HIV fusion inhibitors targeting the gp41 pocket. J. Virol. 86, 589–593. https://doi.org/10.1128/JVI.05066-11.